10,14

Mechanical properties of multi-walled carbon chiral nanotubes and their bundles: *in silico* studies within the density functional theory approach in the tight-binding approximation

© O.E. Glukhova[1,2], P.A. Kolesnichenko[1], M.M. Slepchenkov[1]

[1] Department of Physics, Saratov State University,
Saratov, Russia
[2] Institute of Bionic Technologies and Engineering, Sechenov First Moscow State Medical University
of Ministry of Health of Russia,
Moscow, Russia

E-mail: glukhovaoe@info.sgu.ru

Received May 6, 2025
Revised May 8, 2025
Accepted May 8, 2025

To calculate the electronic structure and mechanical properties of carbon multi-walled chiral nanotubes using quantum methods, original methods have been developed for I) generating super-cells of atomic grids of multi-walled tubes and II) searching for the energetically optimal atomic structure of super-cells comprising tens of thousands of atoms. Using the developed techniques and the DFTB method (the density functional method in the tight-binding approximation), the patterns of mechanical stresses under tension in the range of 0.1−10 % were investigated. It has been established that the elastic moduli (Young's, Poisson's) for bundles of three multi-walled tubes exceed those for individual similar tubes by several times, which makes them promising in the field of developing new materials for encapsulating electronic devices under extreme loads.

Keywords: carbon multi-walled chiral nanotubes, Young's module, the Poissonś ratio, bundles of chiral multi-walled nanotubes, density functional tight-binding (DFTB) method.

DOI: 10.61011/PSS.2025.05.61501.105-25

1. Introduction

The problem of increasing the strength and operation characteristics of structural materials is being currently solved, including with the application of carbon nanotubes (CNT), which are synthesized today at an industrial scale with the controlled diameter and length. The relevance of the solution to this problem depends on the growing requirements to the hardware designed to support and develop the space communications.

CNT-based nanomaterials differ by light weight, super-elasticity, high strength and hardness [1,2]. Such qualities predetermine the use of these materials for packaging of electronic devices operating under extreme conditions. Nanomaterials from CNT include both single-wall CNT (SWCNT), and multi-wall CNT (MWCNT) in their composition. The selection of the most optimal composition of a CNT film (chirality, diameter, number of walls in a MWCNT) depends on pre-modeling with the estimation of mechanical characteristics of MWCNT with various quantity of walls.

They have been developing atomistic models of CNTs and their bundles, studying their structural and mechanical stability since the beginning of 2010s [2–5]. To overcome the problem of modeling polyatomic CNTs, MWCNTs and their bundles, different approaches are used: building coarse-grained models [6–8]; building full-atom models based on small diameter SWCNTs with the same chirality indices [9]. In paper [9] the authors research the strain behavior of the SWCNT bundle (3,3) exposed to stretching with the account of the different value of the SWCNT twisting angle inside the bundle. Besides, a bundle model is considered, which consists of nineteen parallel-oriented SWCNTs, which are twisted into a „small rope" at angles 0, 10 and 20°, and the patterns of mechanical properties are then studied on these models when the structure is stretched. The other paper [10] cites the research of the dynamic response of SWCNT bundles with chirality indices (6,6) under a mechanical shock with the help of the molecular dynamics and power field AIREBO-M in LAMMPS software suite. Currently there are no models of bundles from MWCNTs, which include CNTs of various chirality in their composition. Such research *in silico* requires substantial computing resources, experimental research is very fine from the position of its implementation with minimum error. Computer study of the bundle mechanical properties was successfully conducted for a case of a package from non-chiral SWCNTs, which applied the empirical approach and molecular-dynamic modeling. Experimental research was implemented for the layers from CNTs, which were evenly stretched along the axis of the tubes, and also for individual tubes, which were exposed to twisting [11]. The patterns of Young's modulus variation depending on the aspect ratio were studied for individual CNTs [12,13].

The objective of this paper — is to identify the patterns in variation of mechanical properties (in particular, Young's and Poisson's moduli) using quantum-mechanical approaches: 1) with increase of the quantity of chiral CNTs within a MWCNT with the internal diameter of the channel $\sim 4-5$ nm; 2) upon combination of MWCNTs of various layering with the internal diameter of the channel $\sim 4-5$ nm into bundles.

2. Method of study

All theoretical studies were conducted using the SCC DFTB method (self-consistent-charge density-functional tight-binding method) [14], which provides for high accuracy of calculations of energy and electron characteristics on the background of using polyatomic supercells. The total energy of the structure is determined by the following expression:

$$E_{\text{tot}} = E_{\text{band}} + E_{\text{scc}} + E_{\text{rep}}, \quad (1)$$

where E_{band} — energy of occupied electron states, E_{scc} — energy of electron interaction, E_{rep} describes energy of atom nuclei repulsion. The first term energy — E_{band} is calculated by summing the Hamiltonian's eigenvalues ε_v, corresponding to the filled electron states. The second term — energy E_{scc}, takes into account the change of the electron density in interaction of atoms of various chemical elements. This energy depends on redistribution of electron charge density estimated using Mulliken's method, and Coulomb interaction, including exchange-correlation interaction and Hubbard's parameters. The third term — phenomenological energy E_{rep}, energy of repulsion of two atom nuclei, not taken into account in estimation of energies E_{band} and E_{scc}. The value of energy E_{rep} is presented in the form of a sum of paired repulsed potentials between atoms i, j:

$$E_{\text{rep}} = \sum_{i<j} V_{\text{rep}_{i,j}}(r_{i,j}), \quad (2)$$

where potential $V_{\text{rep}_{i,j}}$ is specified with the sum of polynomial functions:

$$V_{\text{rep}}(r) = \sum_{p=2}^{6} c_p (r_{\text{cut}} - r)^p. \quad (3)$$

Here r_{cut} — cutoff radius, i.e. the distance from this atom to the adjacent one, where the energy of interatomic interaction is still non-zero (as this distance is exceeded, it is assumed that atoms do not interact), coefficients c_p and degrees p specify the shape of the spline determining the properties of interatomic interaction potential. Potential $V_{\text{rep}_{i,j}}$ is short-acting and decreasing as the distance between atoms increases. This paper used a basic Slater–Koster set (sk-files) pbc-0-3 [15]. Dispersion interaction between the tubes within an MWCNT was taken into account using the Lennard–Jones potential.

To obtain energy favorable atomic configuration of supercells, the full energy minimization was performed by all coordinates of all atoms, and by all lengths of translation vector of super-cell at electron temperature 300 K. A 3D-periodic cell was used, its dimensions were determined by the value of the transmission vector along the CNT axis (bundle made of CNT), which was sent along the axis Y of the Cartesian coordinate system, in two other dimensions the cell size was 100 nm. To correctly bypass the first Brillouin zone, Monkhorst–Pack grid was used with discretization $3 \times 1 \times 3$. To minimize full energy the conjugate gradients method was used. Condition for full energy minimum achievement was force acting on atom, its value shall not exceed 10^{-4} eV/atom.

The Young's modulus was calculated using the formula from the Hooke's law:

$$Y = \frac{2\Delta E_{\text{tot}}}{\Delta V} \frac{l}{\Delta l}, \quad (4)$$

where in the numerator the change of full energy from stretching/compression, in the denominator — volume change, $\Delta l/l$ — strain. The mechanical stress is calculated, accordingly, using the following formula:

$$\varepsilon = \frac{2\Delta E_{\text{tot}}}{\Delta V}. \quad (5)$$

Poison's ratio of SWCNT, MWCNT and their bundles is calculated using the change of the effective diameter of the corresponding cylindrical and polyhedral structures made of tubes:

$$\mu = -\frac{\Delta d_{\text{eff}}}{d_{\text{eff}}} \frac{l}{\Delta l}, \quad (6)$$

where the effective diameter means the averaged value of diameter for MWCNT and the value of the bundle contour diameter — diameter of circumference, where the outer contour of the nanotube bundle is fitted.

3. Results

3.1. Quantum-mechanical calculations of chiral SWCNTs moduli of elasticity, comparison to experimental data

For some chiral CNTs studied experimentally they performed calculations of stress–strain ratios to verity the estimated moduli of elasticity. A tube may be presented in the form of a cylinder with a certain radius r and angle α, which define the position of each atom on a cylindrical surface. Such approach makes it possible to generate an atomic grid of CNT at any chirality. Figure 1, *a* shows a CNT fragment in the form of a cylindrical surface, atoms of which are specified by radius r and angle α. All atoms are in circumferences with the center on the CNT axis. Figure 1, *b–c* presents the results of quantum-mechanical studies of stress–strain dependences for two chiral tubes (15,6) and (16,4) — black dots. The same figures present the results of experimental studies obtained in paper [16], they are marked with red crosses. Table 1 presents the results of Young's modulus estimates and

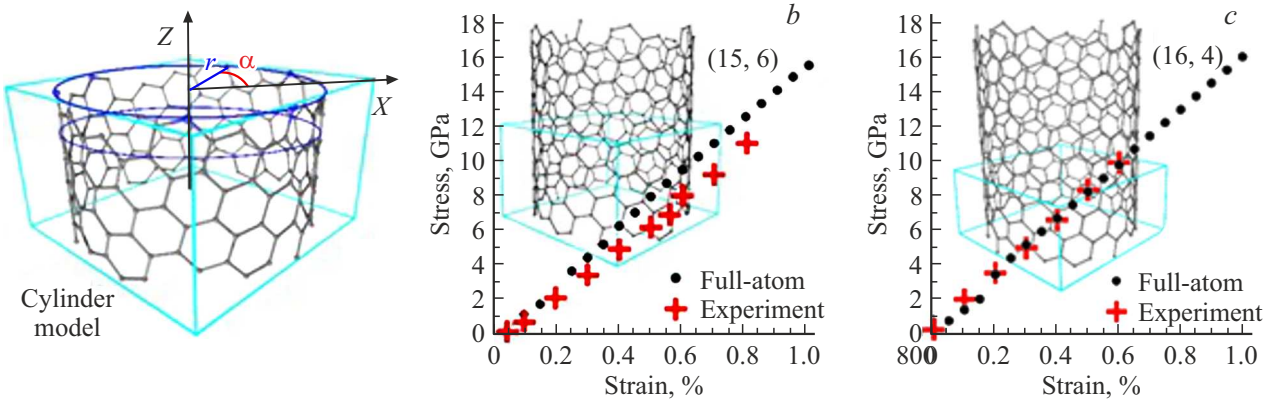

Figure 1. Atomistic models and strain properties of chiral nanotubes: *a* — CNT model in the form of a cylinder with radius *r* and angle of atom location on the cylinder α; *b* — ratio of stress–strain for CNT (15,6); *c* — ratio of stress–strain for CNT (16,4).

Table 1. Comparative parameters of nanotubes

OUNT	*in silico*		Experiment [16]		Error
	D, nm	Y, TPa	D, nm	Y, TPa	$\lvert\Delta Y\rvert/Y$, %
(14,1)	1.150	1.92	1.137	2.17 ± 0.036	11.5
(16,4)	1.449	1.61	1.435	1.63 ± 0.034	1.22
(15,6)	1.482	1.46	1.467	1.34 ± 0.035	8.95

measurement data, which confirm that quantum-mechanical calculations of Young's modulus are within the error of $\sim 7\,\%$ compared to the averaged measured values.

3.2. MWCNT with internal diameter of channel $\sim 4-5$ nm

MWCNT type tubes are characterized by two parameters: diameter of the internal channel and number of layers — walls formed by tubes. For example, in paper [17] it is shown that the specific internal channel of MWCNT is a tube with diameter of $\sim 4-6$ nm, and the number of layers may reach three and more. This paper adopted a MWCNT model as the basis with the internal channel ~ 4 nm and three walls. As we know, synthesized CNTs have the length of several micrometers/millimeters. Atomistic CNT models may not be characterized by the same length due to polyatomic nature of such structures, therefore it is necessary to generate super cells, the periodic boundary conditions of which automatically provide for the research of infinitely long 1D-nanostructures, the properties of which may be compared to the synthesized CNTs of micron/micrometer length. The problem of generation of atomic lattices of such super cells is the complexity to select single-wall CNTs within MWCNT, which differ by chirality and, accordingly, type of conductivity. Intermural spacing in MWCNT at the same time must meet the value ~ 3.4 Å. Therefore, when MWCNT super cells are created, it is necessary to comply with the following mandatory conditions: 1) intramural spacing; 2) various chirality of CNT; 3) identical values of transmission vectors along CNT axes, which finally defines the MWCNT transmission vector.

The original method is developed for generation of atomic lattices of MWCNT with the specified diameter of the internal channel. The mathematical essence of the method consists in the following:

1) A sample of chirality indices is assigned (m, n), for example, in the range of $(1-100)$, and the diameter of the internal channel D is specified as the main determinant parameter. The value of the intermural spacing is specified within the limits of $\sim 3.3-3.5$ Å, also the number of walls is specified within MWCNT;

2) All potential options are estimated for the combinations of chiral tubes (m, n) within MWCNT with the specified number of the walls and the specified intramural spacing. Accordingly, diameters of tubes D and vectors of transmissions T_C are calculated:

$$D = \frac{0.246\sqrt{n^2 + nm + m^2}}{\pi}, \qquad (7),$$

$$T_C = \frac{\sqrt{3}C}{gcm(n, m)}, \quad C = 0.246\sqrt{n^2 + nm + m^2}, \qquad (8)$$

where gcm — greatest common divisor (GCD);

3) Structures, parameters of which meet the specified ones most, are selected from the produced set of all possible MWCNT models. At this stage the value of the diameter of the internal channel D may vary within several percents and may not strictly comply with the initially specified value. The value of intramural spacing may also vary within 3.4 ± 0.2 Å. However, the transmission vector T_C for all SWCNTs within MWCNT must coincide within very narrow limits, not exceeding 1 %, since this is exactly the parameter that determines the periodic boundary conditions for the MWCNT model super cell. The intermural spacing may be corrected effectively in process of optimization of the super cell structure as a result of accounting of the

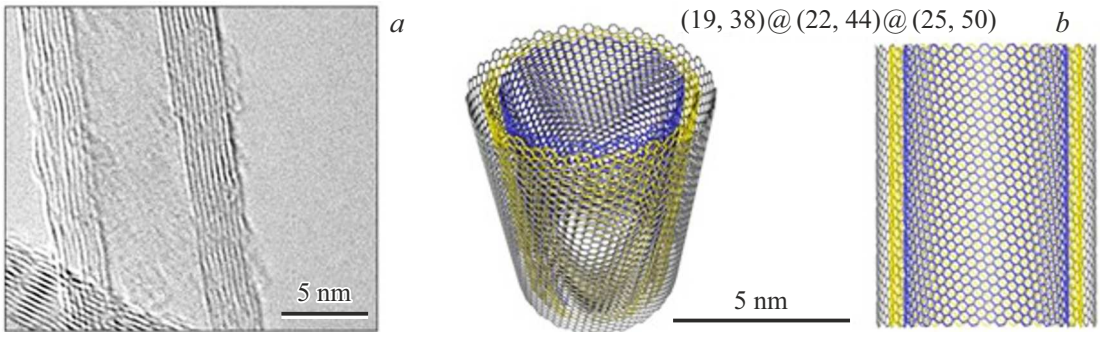

Figure 2. Multi-wall CNTs: TEM image of MWCNT from ten nanotube walls [17]; atomistic model of MWCNT from three nanotuble walls with the distance between the walls $\sim 3.3-3.5$ Å (two angles — in 3D-image and perspective, and in 2D-section).

Table 2. Geometric and energy characteristics of CNTs

CNT	Number of atoms	T_C, Å	D, Å	E_{tot}, eV/at	E_{vdW}, eV/at
(19,38)	532	11.358	39.660	−47.085	–
(22,44)	616	11.357	45.922	−47.091	–
(25,50)	700	11.358	52.188	−47.092	–
(19,38)@(22,44)	1148	11.352	39.407/46.192	−47.127	0.222
(22,44)@(25,50)	1316	11.352	45.681/52.446	−47.128	0.223
(19,38)@(22,44)@(25,50)	1848	11.349	39.240/45.835/52.647	−47.141	0.207

dispersion interaction between the SWCNT walls within MWCNT. And the correction of value T_C is only permissible to a small extent to avoid inelastic extension/compression of SWCNT.

Multi-wall CNTs are characterized by large diameter of the internal channel $D \sim 4-7$ nm and the number of the walls within ten (Figure 2, *a* shows the image of such nanotube). This paper builds the model of three-/two-wall MWCNTs with $D \sim 4-5$ nm. Using the described method, the optimal structures are identified: (19,38)@(22,44), (22,44)@(25,50) and (19,38)@(22,44)@(25,50). Figure 2 presents the TEM image of the tube and atomistic models of the three-wall MWCNT (at two angles). Restriction to the three-wall model is due to the considerable computing resources necessary for quantum research of MWCNT electronic properties. A super cell of the produced atomistic model of MWCNT includes 1848 atoms with the length of the transmission vector ~ 11.273 Å (prior to optimization). Single-wall tubes were optimized within MWCNT, a two-wall and a three-wall ones. Geometric parameters of the tubes, full energy and energy of van der Waals interaction of MWCNT walls (given per atom) are specified in Table 2. The values of diameters of the internal and external tubes were given for MWCNT. Two-/three-wall tubes are beneficial from the energy point of view compared to SWCNT, but the three-wall tube is more stable by energy.

The mechanical properties of the tubes were studied under gradual extension by fractions of percent until 1 % extension was achieved. At each stage of extension, the nanostructure was optimized, and stress values were calculated (5). The results are provided in Figure 3: *a*) for three SWCNTs; *b*) two two-wall tubes and *c*) three-wall tube. Inserts of Figure 3, *b* and 3, *c* show atomistic models of MWCNT (walls are marked with different colors for better visualization, a super cell is marked with the green box). For SWCNT the extension step was 0.05 %, for MWCNT — 0.1 %. A certain „phase transition“ was found for all tubes, where stress−strain ratio changes step-wise with the change of the inclination angle. Such transition for all tubes is observed within one percent of extension. Thorough analysis of experimental data confirms such nature of the change in the stress−strain ratio [16]. Table 3 provides values Y for two strain ranges. An interesting pattern was found: „phase transition“ in SWCNT occurs in extension of 0.55−0.65 %, in two-wall ones this threshold is less than ~ 0.45 %, in a three-wall tube it is even less than ~ 0.35 %. Possibly, as the number of MWCNT walls increases to ten and more, this threshold will decrease to two decimal places of a percent or will totally disappear. Table 3 presents the values of the Young's modulus (4) in two ranges of extension and the Poison's ratio (6), calculated for the case of extension at 1 %. Tubes (19,38)@(22,44) and (19,38)@(22,44)@(25,50) are characterized with the best parameters.

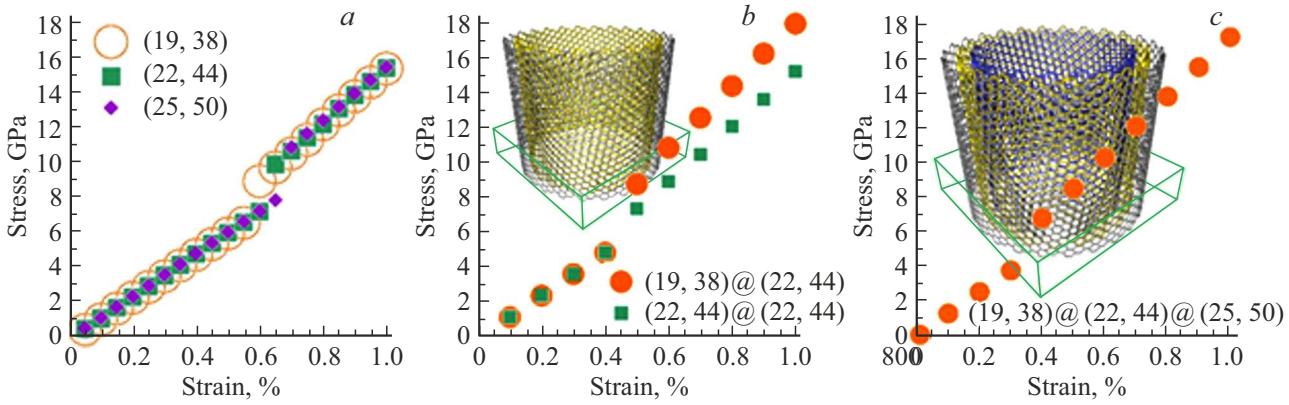

Figure 3. Curves of stress–strain ratio for: *a* — SWCNT, *b* — two-wall CNTs, *c* — three-wall CNTs (on inserts — models of tubes, a super cell is shown in the green box).

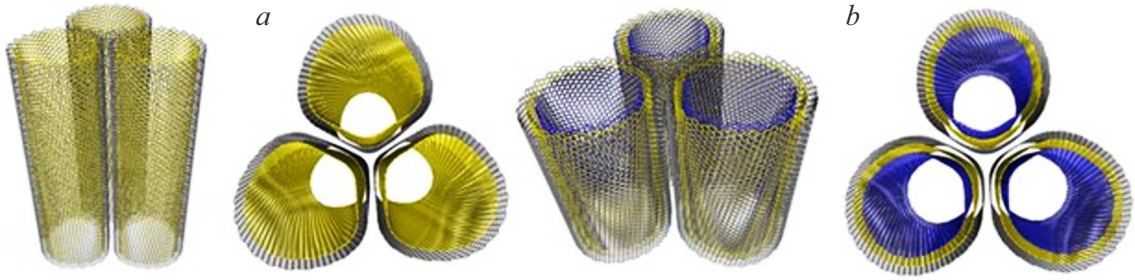

Figure 4. Atomistic models of MWCNT: *a* — (19,38)@(22,44); *b* — (19,38)@(22,44)@(25,50).

Table 3. SWCNT and MWCNT moduli of elasticity

CNT	Y, TPa		μ (for 1 %)
(19,38)	1.158 (0–0.55 %)	1.531 (0.60–1 %)	0.273
(22,44)	1.186 (0–0.60 %)	1.538 (0.65–1 %)	0.277
(25,50)	1.207 (0–0.65 %)	1.550 (0.70–1 %)	0.282
(19,38)@(22,44)	1.215 (0–0.45 %)	1.788 (0.50–1 %)	0.284
(22,44)@(25,50)	1.221 (0–0.45 %)	1.498 (0.50–1 %)	0.288
(19,38)@(22,44)@(25,50)	1.232 (0–0.35 %)	1.714 (0.40–1 %)	0.266

3.3. Bundles from MWCNT

Atomistic models of thin bundles are built from two-/three-wall MWCNTs. Due to polyatomic nature of super cells, only bundles of three MWCNTs were considered, which form a triangular secondary structure. Models of three bundles are built from the same tubes — two-wall ones (19,38)@(22,44) and (22,44)@(25,50), and a three-wall one (19,38)@(22,44)@(25,50), for which the super cells of bundles are produced as a result of optimization with the vectors of transmissions with length of 11.351, 11.352 and 11.349 Å, respectively. The number of atoms in the super cells is 3444, 3948 and 5544 atoms, respectively. The tube-to-tube distance in the bundles is 3.34–3.42 Å. Figure 4 shows the fragments of two bundles: *a*) from tubes (19,38)@(22,44) with length of 11 super cells; *b*) from MWCNT (19,38)@(22,44)@(25,50) with length of 7 super cells.

To calculate the Young's modulus (4, the algorithm was developed to calculate the area of the bundle cross section, which consists in performance of several actions (Figure 5): 1st step — transition from the cylinder to the contour of the bundle tubes in the plane of the cross section relative to the tube axis; 2nd step — building an outer (marked with red) and an inner (blue) contours for each tube by displacement along the radius vector to the distance of the van der Waals radius of atom outwards (for the outer tube) and inwards (for the inner tube); 3rd step — all contours of source tubes

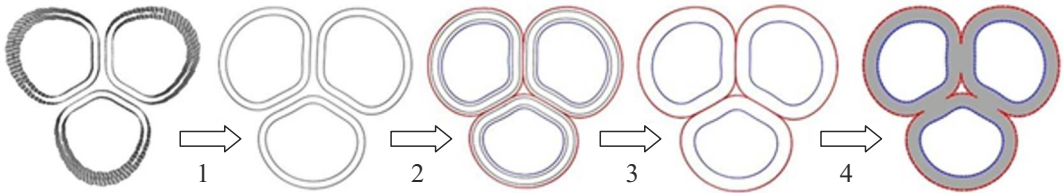

Figure 5. Transformation of the MWCNT bundle structure to calculate the surface area of the bundle cross section (the produced surface area of the bundle is marked with grey).

Table 4. SWCNT and MWCNT moduli of elasticity

Bundle composition	$D1$, Å	$D2$, Å	$D3$, Å	S, nm^2	Y, TPa	d_{eff}, Å	μ
(19,38)@(22,44)	39.407	46.064	–	27.23	2.49	101.24	6.40
(22,44)@(25,50)	–	45.681	52.446	38.30	2.28	105.70	6.38
(19,38)@(22,44)@(25,50)	39.240	45.835	52.647	43.60	2.52	116.90	6.50

are removed; 4th step — parts of touching outer contours are removed, which results in the final form of the bundle section in the plane, perpendicular to its axis (in Figure 5 the produced surface area of the bundle section is marked with grey).

Calculations of the Young's modulus and Poison's ratio were carried out only for the case of 1% extension, since the optimization of the atomistic structure of the bundle from MWCNT requires considerable computing resources, which limits the circle of DFTB of the studied secondary structures from MWCNT. The obtained results are presented in Table 4, where diameters of the tubes are shown within the bundle ($D1, D2, D3$), the surface area of the bundle figure S in the cross section, Young's modulus, effective diameter of the bundle d_{eff} and Poison's ratio.

4. Conclusion

The original method is developed for generation of atomic lattices of MWCNT with the specified diameter of the internal channel. The method makes it possible to determine any combinations of MWCNTs at the specified diameter.

MWCNT models were built with the internal channel $\sim 4-5$ nm, and their mechanical properties were studied, and properties of bundles made thereof, within three MWCNTs. A new effect was specified — phase transition of MWCNT upon tension at $0.35-0.65$ %, accompanied with the step-wise increase of the Young's modulus by $\sim 30-45$ %. The transition strain value depends on the quantity of the MWCNT walls, the more is the number of the walls, the less is the transition strain value: for SWCNT — $0.55-0.65$ %, two-wall ones — 0.45 %, a three-wall one — 0.35 %. Besides, the highest value of the Young's modulus was found in a two-wall and a three-wall tube. The Poison's ratio increases as the SWCNT diameter increases, the same trend is maintained for two-wall CNTs.

Bundles from two-/three-wall CNTs exceed by Young's modulus all the studied tubes, its value exceeds by 41 % the values of the Young's modulus of the most elastic two-wall tube and exceeds two TPa. Besides, the Poison's ratio is several times higher than that of individual MWCNTs and is $\sim 6.3-0.05$.

The developed method for generation of atomic lattices of MWCNT and the method to calculate the moduli of elasticity of MWCNT bundles will make it possible to predict the secondary structures from nanotubes with the controlled mechanical properties.

Funding

The study was carried out within the grant of the Russian Science Foundation (project No. 25-29-00963).

Conflict of interest

The authors declare that they have no conflict of interest.

References

[1] A.V. Eletskiy. UFN **177**, 233–274 (2007). (in Russian).
[2] Yu.A. Baimova, R.T. Murzaev, S.V. Dmitriev. FTT **56**, *10*, 1946 (2014). (in Russian).
[3] C.H. Wong, V. Vijayaraghavan. Comput. Mater. Sci. **53**, *1*, 268–277 (2012).
[4] A.M. Beese, X.D. Wei, S. Sarkar, R. Ramachandramoorthy, M.R. Roenbeck, A. Moravsky, M. Ford, F. Yavari, D.T. Keane, R.O. Loutfy, S.T. Nguyen, H.D. Espinosa. ACS Nano **8**, *11*, 11454–11466 (2014).
[5] C.F. Cornwell, C.R. Welch. Molecular Simulation, **38**, *13*, 1032–1037 (2012).
[6] X. Liu, W. Lu, O.M. Ayala, L.-P. Wang, A.M. Karlsson, Q. Yang, T.-W. Chou. Nanoscale **5**, *5*, 2002–2008 (2013).
[7] G. Gul, R. Faller, N. Ileri-Ercan. Biophys. J. **122**, *10*, 1748–1761 (2023).

[8] B. Arash, H.S. Park, T. Rabczuk. Compos. B: Eng. **80**, 92–100 (2015).
[9] D. Zhao, X.Q. Wang, L.-H. Tam, C.L. Chow, D. Lau. Thin–Walled Struct. **196**, 111536 (2024).
[10] Y. Li, B. Zhang. Diam. Relat. Mater. **140, Part A,** 110476 (2023).
[11] H. Wei, H.Z.J. Ting, Y. Gong, C. Lü, O.E. Glukhova, H. Zhan. Nanomaterials (Basel), **12**, *5*, 760 (2022).
[12] J-G. Kim, D. Suh, H. Kang. Curr. Appl. Phys. **21**, 96–100 (2021).
[13] M.V. Il'ina, O.I. Il'in, A.A. Konshin, A.A. Fedotov, O.A. Ageev. IOP Conf. Ser.: Mater. Sci. Eng. **443**, 012010 (2018).
[14] G. Budiutama, R. Li, S. Manzhos, M. Ihara. J. Chem. Theory Comput. **19**, *15*, 5189–5198 (2023).
[15] Density Functional Tight Binding. Electronic source. https://dftb.org (date of access: 2025-04-25).
[16] J. Sun, X. Zhang, Y. Wang, M. Li, X. Wei, H. Liu, W. Zhou. Nano Res. **17**, 7522–7532 (2024).
[17] A.Y. Gerasimenko, E. Kitsyuk, U.E. Kurilova, I.A. Suetina, L. Russu, M.V. Mezentseva, A. Markov, A.N. Narovlyansky, S. Kravchenko, S.V. Selishchev, O.E. Glukhova. Polymers **14**, *9*, 1866 (2022).

Translated by M.Verenikina